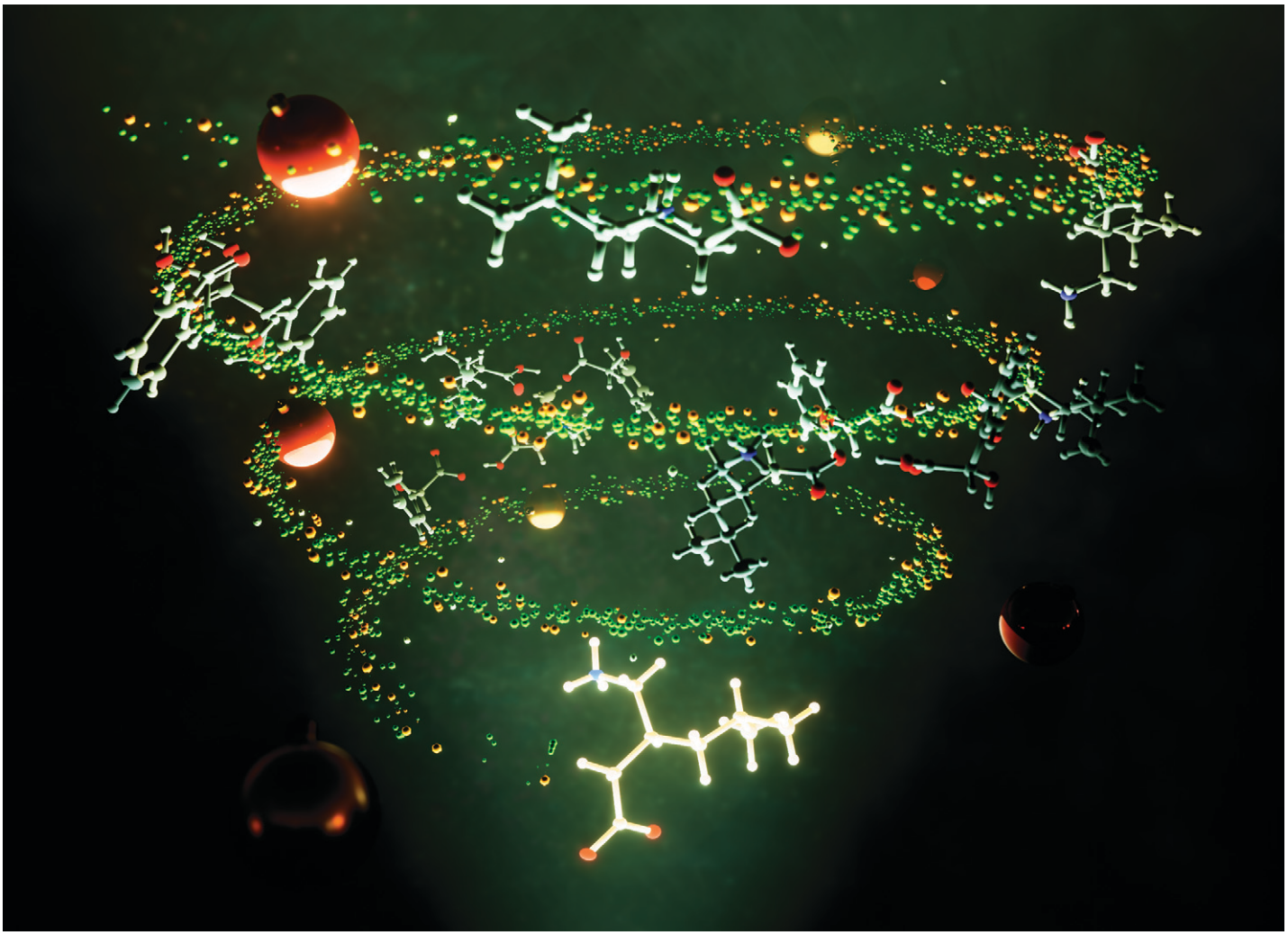

Showcasing research from Dr. Vera Vasylyeva's laboratory, Department of Structural and Inorganic Chemistry, Heinrich-Heine University Duesseldorf, Germany.

Co-crystals of zwitterionic GABA API's pregabalin and phenibut: properties and application

A set of multicomponent crystals of chiral, pharmaceutically active γ-amino butanoic acid derivatives pregabalin and phenibut is presented. APIs and co-formers mandelic and malic acid are in a similar pKa-range, which enables formation of either salts or co-crystals. With a detailed analysis of their crystal architecture, thermal properties, solubilities and lattice energies we bring the pieces of a puzzle together. This allows a development of an improved top-down racemic separation process. Mechanochemically synthesised salt/co-crystal mixtures of pregabalin:mandelic acid can be easily separated with water and acetone to give enantiopure pregabalin.

As featured in:

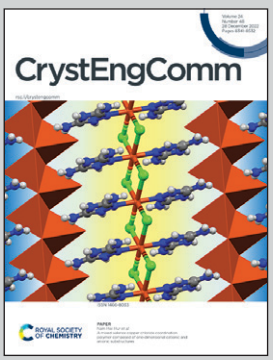

See Vera Vasylyeva *et al.*, *CrystEngComm*, 2022, **24**, 8390.

ROYAL SOCIETY OF CHEMISTRY

rsc.li/crystengcomm

Registered charity number: 207890

CrystEngComm

PAPER

View Article Online
View Journal | View Issue

Cite this: *CrystEngComm*, 2022, **24**, 8390

Received 13th October 2022,
Accepted 17th November 2022

DOI: 10.1039/d2ce01416e

rsc.li/crystengcomm

Co-crystals of zwitterionic GABA API's pregabalin and phenibut: properties and application†

Daniel Komisarek, Takin Haj Hassani Sohi and Vera Vasylyeva *

We present several multicomponent crystalline species formed by zwitterionic GABA analogues pregabalin and phenibut. These compounds are evaluated based on their crystal structure in congruence with properties such as melting behaviour, solubility, and lattice energies. Furthermore, it is discussed how major property distinctions between a homo- and heterochiral co-crystalline system enable enantiopurification of pregabalin.

1 Introduction

In crystal engineering of active pharmaceutical ingredients (APIs) the enhancement of attributes such as solubility or drug stability is an ongoing task. Various approaches are used to identify influences on crystal properties and increasingly more sensitive ways are developed to synthesize a desired target product.[1–10] In many cases, thermodynamic factors such as lattice energies play an important role in the outcome of an attempted crystallization. Computational methods based on density functional theory (DFT) as well as force field applications have proven to be useful in determining energetic properties of single as well as multicomponent species.[11–15] A common approach in using DFT-methods for lattice energy calculations is to compare energies of larger crystalline slabs to energy sums of occurring crystallographically independent molecules in the unit cell. However, differing molecular charges can make that task difficult. Aside from their effect on energy calculations, molecular charges build a basis for the classification of crystalline solids, for example as either a salt or a neutral co-crystal. Childs *et al.* describe the salt-cocrystal continuum in their 2007 contribution, evaluating molecular influences of the co-formers and their acidity as important factors for the charge status of the received product.[16] In 2010 Braga *et al.* coined the term ionic co-crystal. After describing multicomponent crystalline entities composed of neutral barbituric acid and various alkali bromides or caesium iodide, their publication closes with the suggestion to further examine enthalpic and entropic contributions *via* theoretical evaluations.[17] They brought up the topic again in 2018, focussing on inorganic and organic co-crystalline systems, highlighting pharmaceutical and agricultural applications and especially the enantiomeric resolution of racemates as interesting uses.[18] Additional discussions on the influence of ionicity on structure, properties or formation of co-crystalline species containing various charged molecular species have been conducted over the years,[19–21] also in conjunction with organic/organic multicomponent crystalline entities. Various definitions for such structures have been proposed.[22–26] As the established terminology has found acceptance in the community,[27–30] methods to explicitly distinguish between salts and ionic co-crystals were designed.[31,32] Next to varying molecular charges and acidity, a further molecular influence which can impact crystalline structure and lattice makeup is molecular chirality.[18,33,34] Mandelic acid and its derivatives have shown remarkable chirality-based influences on co-crystalline systems when used as co-formers.[35–37] In the past, several processes were patented that amongst other compounds use mandelic acid to separate *e.g.* (*S*)-pregabalin ((*S*)-4-amino-3-isobutylbutanoic acid) from its (*R*)-enantiomer. (*S*)-Pregabalin, the eutomer, which is the enantiomer that shows the desired pharmaceutical properties, and (*R*)-pregabalin, its distomer, with no or undesired pharmaceutical effects, can be separated *via* co-crystal formation with mandelic acid and subsequent co-former removal.[38–44] Pregabalin is a pharmaceutically active γ-amino butanoic acid (GABA) derivative with a considerable amount of uses as an API. Pregablin remained a staple treatment API for such diseases as epilepsy, neuropathic pain and anxiety disorders over the years since its release.[45–54] It is chiral, shows zwitterionic charges on its GABA-subunit and being an amino acid is slightly acidic. A further related nootropic and anxiolytic drug is phenibut ((*RS*)-4-amino-3-phenylbutanoic acid) where the (*R*)-enantiomer is the eutomer,[55–57] that has fallen out of favour for its abuse potential.[58–62] As another

Department of Inorganic and Structural Chemistry I, Laboratory for Crystal Engineering, Heinrich-Heine-University, Universitaetsstraße 1, 40225 Duesseldorf, Germany. E-mail: vera.vasylyeva-shor@hhu.de

† Electronic supplementary information (ESI) available. CCDC 2170100–2170108. For ESI and crystallographic data in CIF or other electronic format see DOI: https://doi.org/10.1039/d2ce01416e

GABA-derivative, it also contains a zwitterionic subunit, poses chirality in C3 and is also a weakly acidic amino acid. In the present work various co-crystalline embodiments of enantiomers of pregabalin (**1**) and racemic phenibut (**2**) with co-formers mandelic acid (**3**) and malic acid (**4**) are examined (Scheme 1). Pregabalin exhibits an unusual behaviour to form a zwitterionic/neutral co-crystal with mandelic acid as first described by Samas *et al.* in 2007,[63] or a system composed solely of charged molecules depending on whether a homo- or heterochiral set of co-formers is co-crystallized. For comparison a set of multicomponent systems of pregabalin with malic acid and phenibut with mandelic acid is presented to show that the described behaviour is unique for pregabalin and mandelic acid only. Molecular influences such as zwitterionicity, chiral information and compound acidity in multicomponent entities are discussed in congruence with structural makeup and intermolecular interactions, especially hydrogen bond (HB) as well as properties like melting behaviour, solubility in aqueous medium and lattice energies. These findings are then applied to explain how the enantiopurification of pregabalin according to the established process with mandelic acid can be understood and improved on. It is shown how a specific set of molecular and structural influences enables a useful application.

2 Experimental and computational methods

Single-crystal X-ray diffraction

Suitable single crystals were selected from the sample and mounted on a cryo-loop under protective oil. Diffraction data were recorded with a Rigaku XtaLAB Synergy S diffractometer with Hybrid Pixel Arrow detector and a PhotonJet X-ray source using Cu-Kα radiation (λ = 1.54182 Å) at 100.0 ± 0.1 K with ω-scans. Data reduction and absorption correction were conducted on CrysAlisPRO v. 42 software, numerical absorption correction based on Gaussian integration over a multifaceted crystal model and empirical absorption correction using spherical harmonics, implemented in SCALE3 ABSPACK scaling algorithm was used.[64] The single crystal structures were analyzed and refined by using direct methods (SHELXT-2015), full-matrix least-squares refinements on F^2 were performed using SHELXL2017/01 software package.[65,66] Structure solution and refinements were conducted with OLEX2-1.5 software package. Hydrogen atoms were experimentally refined, all esds (except the esd in the dihedral angle between two l.s. planes) are estimated using the full covariance matrix. The cell esds are taken into account individually in the estimation of esds in distances, angles and torsion angles; correlations between esds in cell parameters are only used when they are defined by crystal symmetry. An approximate (isotropic) treatment of cell esds is used for estimating esds involving l.s. planes.[67] Figures were prepared with Mercury software v. 2020.2.0.[68]

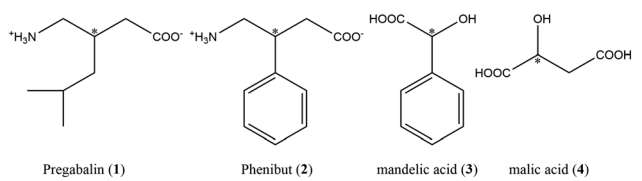

Scheme 1 Compounds used in this work. APIs pregabalin and phenibut as well as coformers mandelic- and malic acid.

Differential scanning calorimetry

Measurements were performed on a Linkam DSC 600 with nitrogen cooling and heating range from −190–600 °C in alumina crucibles.

X-ray powder diffraction

Measurements were performed on a Rigaku Miniflex diffractometer in $\theta/2\theta$ geometry at ambient temperature using Cu-Kα radiation (λ = 1.54182 Å).

Lattice energy calculations

Quantum Espresso (QE) PWSCF v. 6.6 was used to perform periodic calculations based on the Perdew–Burke–Ernzerhof (PBE) functional.[69] The PBEsol basis set was used to describe pseudo potentials. Lattice energies were determined by geometric optimization energies of crystal structures as measured compared to ideal gas states of the participating molecules in a vacuum cluster, similar to the method described by Marchese Robinson *et al.* and Voronin and colleagues.[12,14]

Diffraction quality single crystals

Multicomponent species (*S*,*S*)-**1**:**3**, (*R*,*R*)-**1**:**3**, (*S*,*R*)-**1**:**3**, (*R*,*S*)-**1**:**3**, (*S*,*S*)-**1**:**4**, (*S*,*R*)-**1**:**4** and (*R*,*S*)-**2**:**3** were obtained by co-crystallization of equimolar amounts of co-formers from aqueous solution and subsequent evaporation of the solvent at room temperature. Single crystals of single component species **1** and **2** were obtained by dissolution of powdery substance in aqueous medium and subsequent evaporation of the solvent at room temperature.

Enantiopurification of pregabalin

Two batches of racemic pregabalin hydrate (1.375 g, 7.756 mmol, 1 eq.) and enantiopure mandelic acid (1.180 g, 7.756 mmol, 1 eq.) were co-grinded with a Retsch MM400 ball mill for 40 min at 25 Hz using two 25 mL stainless containers fitted with one PTFE-ball (ø 2 cm) each. The received co-crystalline substance was subsequently washed with water and dried at 45 °C thrice, using 12 mL water in the first wash, 6 mL water in the second wash and 4 mL water in the third washing instance to remove the more soluble heterochiral species. The remaining residue was then stirred in a mixture of 75 mL acetone and 500 μL water for 40 h at room temperature. Filtration of the powdery residue led to enantiopurified pregabalin.

IR spectra

IR-spectra were recorded on the Bruker Tensor 27 Fourier transformed IR device in attenuated total reflectance mode in the range 4000 cm^{-1} to 400 cm^{-1}. Spectra are shown in the ESI.†

^{1}H-NMR spectra

^{1}H-NMR spectra for solubility determination were recorded on a Bruker Avance III NMR-spectrometer at 600 MHz and are shown in the ESI.†

Chemicals

The following chemicals were purchased and used without further purification: (*rac*)-pregabalin hydrate from abcr, (*rac*)-phenibut from BLDpharm, (*S*)-mandelic acid from G&K, (*R*)-mandelic acid from TCI, (*S*)-malic acid from GLENTHAM LIFE SCIENCES and (*R*)-malic acid from BLDpharm. (*S*)-Pregabalin and (*R*)-pregabalin were produced by enantiomeric enrichment from (*rac*)-pregabalin hydrate according to the described procedure.

3 Results and discussion

3.1 Properties

In **1:3**-systems no protonic shift occurs between co-formers if a homochiral (*S*,*S*) or (*R*,*R*) chirality is present, while each molecule becomes formally charged in species of (*S*,*R*) or (*R*,*S*) chirality in pregabalin:mandelic acid co-crystalline entities (Fig. 1). Homochiral forms crystallize isostructurally in regard to each other as do the heterochiral species. Both homo- and heterochiral pairs can be synthesized from solution as well as through neat grinding. Considering **1** and **3** properties, the only significant difference is their molecular chirality. In terms of acidity, a pK_{a1} value of 4.2 is reported for **1** and 3.41 for **3**,[70,71] resulting in a ΔpK_a value of 0.79. According to Childs *et al.* this matches a defined murky area of ΔpK_a = 0–3 for the solid-state protonation where both a salt as well as a co-crystal formation can occur, and additional molecular influences play a role.[16] Similar observations for small structural changes have been conducted in the past. Trifluoro acetic acid becomes an ionic solid at low temperatures when hydrogenated, but a molecular solid when deuterated.[72] It appears likely that the slight change in molecular chirality has a similar energetic effect in **1:3**-species, favouring ionization in heterochiral forms while keeping default charges in homochiral ones. To highlight the uniqueness of the described system, further similar compounds (*S*,*S*)-**1:4**, (*S*,*R*)-**1:4** as well as (*R*,*S*)-**2:3**, were co-crystallized from aqueous solution. Structural characteristics as well as thermodynamic properties were compared between API's and the received multicomponent species. A detailed comparison of hydrogen bonds shows similar characteristics in all compounds regardless of their protonation status (Table 1). The pK_a values should be considered to enhance the understanding of the present HB characteristics. The pK_{a1} value of **4** is 3.40,[73] and that for **2** is 4.44,[74] giving ΔpK_a values of 0.8 for the **1:4**-species and 1.03 for the **2:3** system. All systems are placed in the previously mentioned range of poor definability of the solid-state classification and all form strong – mid

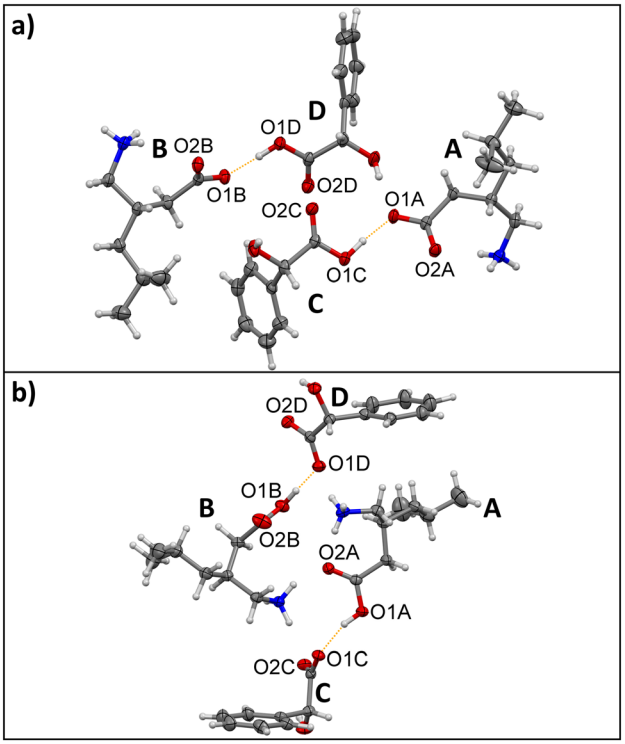

Fig. 1 Illustration of the protonic shift in the asymmetric units of a) homochiral (*S*,*S*)-**1:3** and b) heterochiral (*S*,*R*)-**1:3**. Four crystallographically non-equivalent occurring molecules are marked as A, B, C and D respectively. Proton transfer occurs in (*S*,*R*)-**1:3** between pregabalin A's O1A and mandelic acid C's O1C as well as pregabalin B's O1B and mandelic acid D's O1D. Carbon atoms are depicted in grey, hydrogen atoms in white, nitrogen atoms in blue and oxygen atoms in red. The protonic shift is highlighted in a dotted orange line.

Table 1 An overview of the overall number of hydrogen bonds in the systems, compared to those occurring between two charged subunits. Average, the shortest and the longest HB donor/acceptor distances and their corresponding angles are compared. The average values are calculated for each different occurring HB interaction in the unit cell. Samples composed solely of charged molecules and entries solely involving interactions of charged subunits are written in bold. Carboxylate or ammonium residues in zwitterionic forms are considered charged even though the molecules are overall formally neutral

Sample	Charged HB/all HB	Ø D···A [Å]/D–H···A [°]	Min. D···A [Å]/D–H···A [°]	Max. D···A [Å]/D–H···A [°]
(*S*)-**1**	**3**/3	**2.751/171**	**2.728(0)/171(2)**	**2.771(1)/172(2)**
(*R*)-**1**	**3**/3	**2.752/172**	**2.731(2)/174(2)**	**2.767(2)/172(3)**
(*rac*)-**2**	**3**/3	**2.767/168**	**2.732(3)/160(3)**	**2.795(3)/173(2)**
(*S*,*S*)-**1:3**	**6**/12	2.784/158	2.487(3)/174(2)	**3.036(4)/151(4)**
(*R*,*R*)-1:3	**6**/14	2.818/152	2.489(7)/172(4)	**3.038(2)/148(3)**
(*S*,*R*)-1:3	**4**/14	2.799/145	2.570(3)/179(6)	3.012(3)/121(3)
(*R*,*S*)-1:3	**4**/14	2.797/144	2.570(2)/174(4)	3.006(2)/129(2)
(*R*,*S*)-**2:3**	**3**/7	2.821/151	2.504(2)/175(4)	3.020(2)/117(2)
(*S*,*S*)-1:4	**2**/8	2.827/153	2.446(4)/172(3)	3.154(3)/112(2)
(*S*,*R*)-1:4	**2**/8	2.798/154	2.475(2)/175(3)	3.103(2)/127(3)

strength HBs considering their intermolecular distances. Small ΔpK_a values also facilitate the formation of stronger hydrogen bonds.[75] This shows why the investigated substances behave structurally similar. Even though some of them are composed of overall neutral molecules and some are charged, they all fall into a range of inconclusive pK_a-influence on protonation behaviour, with the oddity present between homo- and heterochiral **1:3**-systems to stay default or protonate/deprotonate apparently solely based on the molecular chirality. Closer examination of HB properties highlights the similarities even further. Except for single species **1** and **2**, where the average HB distance is about 2.75–2.77 Å, the HB average is closer to 2.8 Å in all multicomponent compounds. Interestingly, the shortest interactions never occur between two charged subunits like ammonium and carboxylate. While the shortest HB lengths are observed in malic acid homo- and heterochiral forms (*S*,*S*)- and (*S*,*R*)-**1:4** which are both composed of charged molecules with 2.446(4) Å and 2.475(2) Å, the mandelic acid overall neutral homochiral (*S*,*S*)-**1:3** Å comes closely thereafter with 2.487(3) Å. The corresponding average HB for this system with 2.784 Å is the shortest among the HB averages in multicomponent entities suggesting the strongest overall HB-motif. Average HB distances in multicomponent systems show a rather large deviation from 0.043 Å up to 0.124 Å. On the other hand, single component species **1** and **2** show a more uniform dispersion of HB distances. Here, the average variation is only 0.016 Å, 0.004 Å in the shortest and 0.028 Å in the longest HB. Hydrogen bonds in single-component structures are not exceptionally short, but on average slightly shorter than in the multicomponent systems. This emphasizes that while molecular charges might shift in the described compounds, they all behave structurally similar regarding their HB characteristics, and multicomponent species stay similar to single component APIs. In general, in the most of these systems it is not possible to discern which structural features are influenced by pK_a distinctions and which by molecular influences, but for the **1:3**-species chirality inversion seems to be the most probable cause for the ionization behaviour. Furthermore, ionicity does not appear to have a significant impact on the structural makeup, especially regarding HB lengths and angles. While structurally similar compounds are formed in all investigated species, they do show some significant distinctions in their melting behaviour, solubility and lattice energies (Table 2). As was established in the past, higher melting points correlate with lower solubilities.[76–78] The highest solubility is present in **1:4** that melt below 100 °C with 85 °C for (*S*,*S*) and 95 °C for (*S*,*R*) respectively. In **1:3**-systems the heterochiral forms melt 25 °C lower than their homochiral counterparts and their solubility is about nine times higher at 316 ± 18 g L^{-1} and 307 ± 6 g L^{-1} for (*S*,*R*) and (*R*,*S*) as compared to 37 ± 1 g L^{-1} and 40 ± 4 g L^{-1} for (*S*,*S*)- and (*R*,*R*)-species. All in all, multicomponent systems composed of charged molecules reach far higher solubilities than their zwitterionic or neutral counterparts. This is interesting especially in the case of **1:3** homo- and heterochiral forms. Even though solubility of **3** is about five times higher than that of **1** with 203 ± 3 g L^{-1} and 35 ± 0.4 g L^{-1} or 33 ± 0.3 g L^{-1} respectively, a substantial increase in solubility is not reached in the homochiral co-crystal forms. In co-crystalline entities the solubility is generally linked to several parameters such as co-former solubility, solvent as well as its pH value, co-former pK_a values, co-former complexation by solvent, co-former ratio and ionicity.[79–82] As the same pH-stable solvent conditions were used in all cases and neither the co-former, the co-former ratio nor the co-former pK_a was changed, it is highlighted how the chirality induced change in ionicity possibly affects solvent complexation and thereby increases solubility in heterochiral **1:3**-forms compared to the homochiral systems. It is furthermore surprising that while the melting point in homochiral **1:3**-forms is decreased and **3** is substantially more soluble than **1**, the solubility increase is practically negligible. This indicates that ionicity plays a key-role for the dissolution behaviour. In case of **1:4**-forms, the mentioned criteria for the co-crystal solubility are fulfilled more uniformly. The solubility of **4** with 2061 ± 76 g L^{-1} is exceedingly high compared to that of pure **1**, all components are ionized and a very high solubility of more than 800 g L^{-1} is reached in both cases. In **2:3** an increase of solubility up to 71 ± 3 g L^{-1} is also achieved, which is comparatively low. Here, the increase is most probably due to the large difference between the solubilities of **2** and **3** with 18 ± 1 g L^{-1} and 203 ± 3 g L^{-1} respectively. It is noteworthy that this system is heterochiral, yet here differing chirality does not cause a difference in ionicity as is the case in heterochiral **1:3**-species. This further confirms that ionicity plays an important role in the solubility increase in these compounds, having a larger impact than the co-former solubility alone. Lattice energies do not appear to impact solubility in a significant manner, as all multicomponent species are in a similar range, the lowest values present in homochiral **1:3**-forms with about −320 kJ

Table 2 Overview on the determined melting points, solubilities in aqueous phosphate buffer at pH 6.8 and 37 °C as well as lattice energies calculated with quantum espresso. Bold written samples are composed solely of charged molecules. Mandelic and malic acid solubilities are given in ESI†

Sample	Melting point [°C]	Solubility [g L^{-1}]	E_{lat} [kJ mol^{-1}]
(*S*)-**1**	185	35 ± 0.4	−195.08
(*R*)-**1**	187	33 ± 0.3	−195.17
(*rac*)-**2**	—[a]	18 ± 1	−367.68
(*S*,*S*)-**1:3**	138	37 ± 1	−320.36
(*R*,*R*)-**1:3**	132	40 ± 4	−320.99
(*S*,*R*)-1:3	111	316 ± 18	−304.66
(*R*,*S*)-1:3	105	307 ± 6	−307.77
(*R*,*S*)-**2:3**	150	71 ± 3	−343.23
(*S*,*S*)-1:4	85	>800[b]	−356.66
(*S*,*R*)-1:4	95	>800[b]	−363.05

[a] (*rac*)-Phenibut decomposes prior to melting at about 200 °C, as such no melting point could be determined. [b] The maximum solubility could not be determined. No reliable results could be obtained from the highly viscous substance at higher concentrations.

mol^{-1} and the highest values in **1:4**-systems with −356.66 kJ mol^{-1} in (*S*,*S*) and −363.05 kJ mol^{-1} in (*S*,*R*). As HB-properties are also similar in all investigated compounds, the influence of the charged species on the strength of intermolecular interactions seems to be questionable. While the highest values are present in **1:4**-systems composed of charged molecules, the second most favourable energy is given for **2:3** with −343.23 kJ mol^{-1} composed of zwitterionic and neutral molecules. The calculated lattice energies for the discussed compounds are higher than those established by Marchese Robinson *et al.* for a large number of neutral single component API's,[14] but lower compared to those for ionic liquids containing inorganic ions,[13] and far lower than those for inorganic systems.[83,84] However, the values are slightly higher than values established by Voronin *et al.* for carbendazim maleates.[12] This suggests that (zwitter)ionicity does generally have an influence on lattice energies, even though the final molecular protonation status in multicomponent species of the investigated compounds does not impact structural features meaningfully. The unusually beneficial lattice energy of **2** with −367.68 kJ mol^{-1} might appear too high especially when compared to **1**-forms with about −195 kJ mol^{-1}. However, **2** behaves rather different than **1** in two key aspects: firstly, **2** does not form a stable hydrate as racemic **1** does.[85,86] Contrary to the latter, **2**-hydrate transitions to anhydrous **2** quickly, suggesting a preferable form in the anhydrous species. Furthermore, experimental observations conducted in the presented work suggest a higher stability of **2** as compared to **2:3**. While co-crystalline systems of **1** with the used co-formers form readily and without evidence for impurities under the investigated conditions, the **2:3** system cannot be obtained as reliably. **2:3** single crystals could only be received once; neat co-milling did not work under the chosen conditions and co-crystallization from solution still contains impurities visible in the powder pattern (see ESI†). Therefore, a comparatively beneficial lattice energy seems likely. This might stem from an increased connectivity *via* π-interactions enabled by phenyl-subunits in **2**. Further support for unusually high lattice energy in **2** is given through its melting behaviour. It is the only discussed compound that decomposes without melting at temperatures above 200 °C which indicates strong intermolecular connectivity. To conclude, the comparison of the presented compounds based on the discussed structural and thermodynamic properties uncover their commonalities. They all behave structurally similar as their co-formers are in a specific murky ΔpK_a range that enables formation of salts as well as co-crystals. Some of the chosen systems retain zwitterionic/neutral molecular makeup and some obtain molecular charges. Energetically, they all are in a similar range, posing more beneficial lattice energies than neutral compounds but less favourable ones than organic/inorganic or purely inorganic compounds. However, this border-region in the *salt-co-crystal continuum* can have high impact on properties such as melting and solubility behaviours. The shown compounds that become charged upon co-crystallization melt at lower temperatures and are vastly more soluble than their neutral/zwitterionic counterparts. This specific behaviour seems to largely depend on the molecular chirality in case of homo- and heterochiral **1:3**-forms and the comparatively low lattice energy in **1** enables easy co-crystallization. As **1** is a commercially viable API the presented results can be used to better understand, modify and improve an established crystallization-based enantiopurification processes.

3.2 Enantiopurification of pregabalin

Based on the described findings, a process for the racemic separation of the racemic pregabalin hydrate ((*rac*)-**1**·H_2O) could be improved on and simplified (Scheme 2). Similar enantiopurification methods were previously patented,[38–44] that followed a bottom-up approach in their racemic separation processes. By dissolving varying quantities of (*rac*)-pregabalin hydrate with (*S*)-mandelic acid and subsequently cooling or crystallization *via* vaporization the (*S*,*S*)-species was formed. In the patents it is then removed from solution and further processed. As was shown in the present study the formation of **1:3** is energetically favourable compared to crystallization of **1**. Furthermore, (*S*,*R*)- as well as (*R*,*S*)-**1:3** show ionicity-based increased solubilities compared to the (*S*,*S*)- and (*R*,*R*)-species. In opposition, **1:4**-compounds are prone to form viscous residue instead of crystalline materials which is one of the reasons those are not suitable for the separation process. Due to the energetic favourability as well as mechanic and thermal stability of **1:3**-species they can be prepared in a ball mill *via* mechanochemical synthesis. This enables a top-down approach where the scale depends solely on the largest available milling vessel. By milling of (rac)-**1**·H_2O with either mandelic acid enantiomer (*S*)-**3** or (*R*)-**3** in equimolar amounts a 1 : 1 mixture of the (*S*,*S*)/(*R*,*S*) or (*R*,*R*)/(*S*,*R*) multicomponent systems is formed in good yields (step I in Scheme 2). Missed yield at this point stems from losing some material on the milling vessel walls. As the (*S*,*R*)- and (*R*,*S*)-systems pose an about nine times higher solubility in water compared to their homochiral counterparts they can then be removed by subsequent washing and drying steps with increasingly smaller amounts of water. This approach therefore offers the advantage of quickly producing co-crystalline product and necessitates only low amounts of water to remove the unwanted heterochiral species. To give an example, 4.580 g of co-crystal mixture was produced by milling in step I. After three washing and drying steps with 12 mL, 6 mL and 4 mL water, 1.442 g (62%) of enantiopurified homochiral co-crystal were received in step II. Low amounts of washing water further simplify regaining the missed yield: the lost product can be recrystallized by water vaporization. The washing process can then be repeated with even smaller amounts of water. Our approach does not require further additives like organic solvents, additional acidic or caustic compounds nor is heating

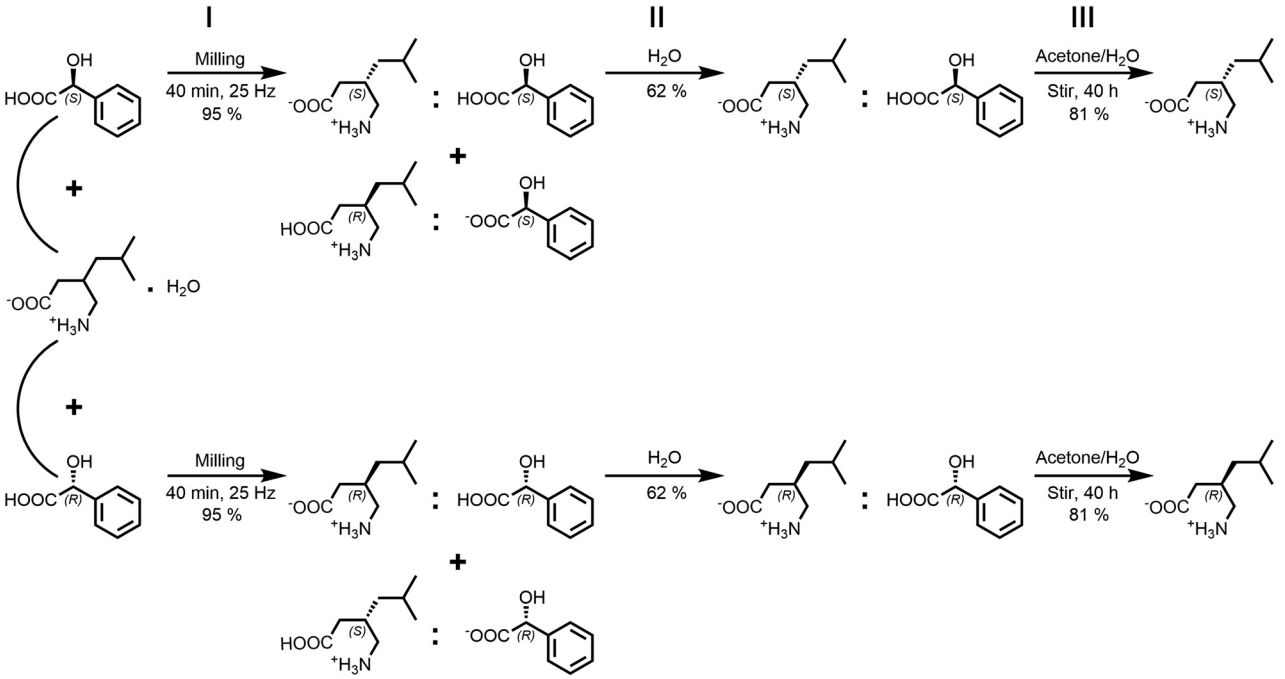

Scheme 2 Steps for the racemic separation of (*rac*)-**1**·H_2O with mandelic acid: step I - mechanochemical co-crystallization, step II - washing powdery product with water and drying the residue, step III - extract mandelic acid by stirring the residue in acetone/water mixture for 40 h.

necessary which is an advantage compared to previously reported procedures. This also allows for an environmentally friendly, low effort process. To separate **3** from **1** in step III a slight variation to the patented process by Pradhan and colleagues,[40] who proposed a number of different separation methods, is introduced. Washed homochiral co-crystalline product is stirred for 40 h in acetone with catalytic amounts of water added. To follow up on the previous example, 1.442 g of powdery co-crystal were put in a glass vessel with 75 mL of acetone and 500 μL of water and stirred for 40 h. The powdery substance was then filtered, washed with additional 20 mL of acetone and 0.612 g (81%) of enantiopurified **1** were received. In contrast to the previously proposed method the stirring process is much longer but does not require heating. Acetone was chosen as it is cheap, easily available and poses less environmental risks than other organic solvents that could be suitable for this process. The proposed enantiopurification can be controlled through powder X-ray diffraction during each step (Fig. 2). The described method relies on property differences unique to the **1**:**3**-systems. Inversion of molecular chirality leads to related multicomponent species that still differ in their key attributes. Higher solubility in one of the received multicomponent species in congruence with the mechanical stability enables the described process for **1**. The previously discussed properties in malic acid systems deem them unusable for this in contrast to **1**:**3**-forms, as **1**:**4**-species preferably form viscous liquids with similar solubilities. On the other end, phenibut co-crystallization with mandelic acid is energetically unfavourable compared to pure **2**-formation. Mechanochemical synthesis under the same herein discussed conditions did not lead to **2**:**3**. Furthermore, **2** does not show chirality dependent varying crystallization products, a trait inherent only to **1**.

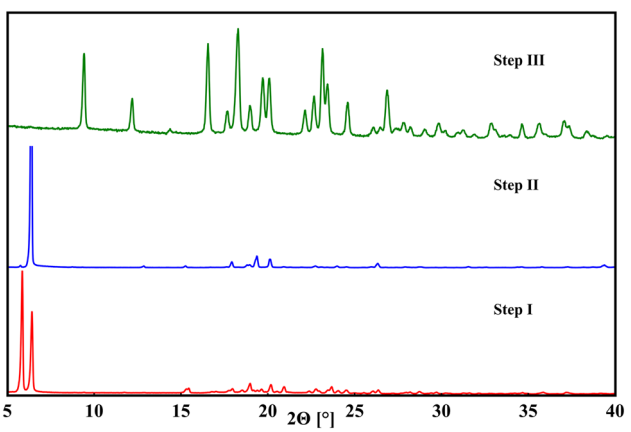

Fig. 2 Powder patterns of products received after enantiopurification process step I (red), step II (blue) and step III (green). In step I, both homo- and heterochiral multicomponent species are present, visible by the two strong diffraction reflexions at 5.9° and 6.4° 2Θ. In step II the heterochiral compound was removed by washing, diminishing the 5.9° signal. In step III, mandelic acid was removed, solely leaving enantiopure pregabalin.

4 Conclusions

In this work we presented an atypical case concerning co-crystallization of zwitterionic APIs of the GABA-family. Multicomponent crystalline species of related compounds

pregabalin and phenibut were characterized regarding their structural and thermodynamic properties. Homo- and heterochiral pregabalin:mandelic acid species exhibit a remarkably different solubility and melting behaviour based on molecular charge differences, even though they are structurally very similar. It was shown that this hardly predictable behaviour occurs in a vague range of the *salt-cocrystal continuum* and can, in this specific case, be attributed to the co-former chirality inversion. It seems likely that this small change in the molecular makeup crosses an energetic barrier needed for ionization when heterochiral co-formers pregabalin and mandelic acid are used. For the given set of compounds, the results indicate that complex multicomponent crystalline species exist on a spectrum and their properties are influenced more impactfully by molecular makeup rather than their crystal structure. It was further presented how investigations of crystal properties in the borderline regions of the spectrum can offer interesting and unexpected results. An optimized and simplified top-down process of (*rac*)-pregabalin hydrate enantiopurification was developed and its functionality was explained by the previously stated properties. This work shows that careful examination of multicomponent systems composed of similar co-formers in areas where multiple molecular and thermodynamic influences compete to determine product properties can lead to fruitful and surprising results.

Author contributions

Conceptualization: Daniel Komisarek & Vera Vasylyeva. Data curation: Daniel Komisarek. Formal analysis: Daniel Komisarek. Funding acquisition: Vera Vasylyeva. Investigation: Daniel Komisarek. Methodology: Daniel Komisarek, Vera Vasylyeva, Takin Haj Hassani Sohi. Project administration: Vera Vasylyeva. Resources: Vera Vasylyeva. Supervision: Vera Vasylyeva. Validation: Daniel Komisarek, Vera Vasylyeva, Takin Haj Hassani Sohi. Visualization: Daniel Komisarek. Writing: Daniel Komisarek. Review & editing: Vera Vasylyeva.

Conflicts of interest

There are no conflicts to declare.

Acknowledgements

We thank PD Dr. Oliver Weingart and Prof. Dr. Rochus Schmid for valuable discussions on theoretical aspects. Computational support and infrastructure was provided by the "Centre for Information and Media Technology" (ZIM) at the University of Duesseldorf (Germany). Funded by the Deutsche Forschungsgemeinschaft (DFG, German Research Foundation) – 440366605. Thanks to the CeMSA@HHU (**Ce**nter for **M**olecular and **S**tructural **A**nalytics@**H**einrich **H**eine **U**niversity) for recording the NMR-spectroscopic data.

References

1 V. Todaro and A. M. Healy, *Drug Dev. Ind. Pharm.*, 2021, **47**, 292–301.
2 M. Trampuž, D. Teslić and B. Likozar, *Chem. Eng. Res. Des.*, 2021, **165**, 254–269.
3 A. Ainurofiq, K. E. Dinda, M. W. Pangestika, U. Himawati, W. D. Wardhani and Y. T. Sipahutar, *Int. J. Res. Pharm. Sci.*, 2020, **11**, 1621–1630.
4 A. J. Al-Ani, C. Herdes, C. C. Wilson and B. Castro-Dominguez, *Cryst. Growth Des.*, 2020, **20**, 1451–1457.
5 D. Chen, Q. Sun, W. Huang and B.-S. Yang, *Cryst. Growth Des.*, 2020, **20**, 2251–2265.
6 L. Schenck, D. Erdemir, L. Saunders Gorka, J. M. Merritt, I. Marziano, R. Ho, M. Lee, J. Bullard, M. Boukerche and S. Ferguson, *et al.*, *Mol. Pharmaceutics*, 2020, **17**, 2232–2244.
7 A. F. Shunnar, B. Dhokale, D. P. Karothu, D. H. Bowskill, I. J. Sugden, H. H. Hernandez, P. Naumov and S. Mohamed, *Chemistry*, 2020, **26**, 4752–4765.
8 H.-L. Cao, J.-R. Zhou, F.-Y. Cai, J. Lü and R. Cao, *Cryst. Growth Des.*, 2019, **19**, 3–16.
9 S. Chattoraj and C. C. Sun, *J. Pharm. Sci.*, 2018, **107**, 968–974.
10 E. Hadjittofis, M. A. Isbell, V. Karde, S. Varghese, C. Ghoroi and J. Y. Y. Heng, *Pharm. Res.*, 2018, **35**, 100.
11 F. Yang, C.-X. Yan, X. Yang, D.-G. Zhou and P.-P. Zhou, *CrystEngComm*, 2017, **19**, 1762–1770.
12 A. P. Voronin, A. O. Surov, A. V. Churakov, O. D. Parashchuk, A. A. Rykounov and M. V. Vener, *Molecules*, 2020, **25**, 2386.
13 U. P. Preiss, D. H. Zaitsau, W. Beichel, D. Himmel, A. Higelin, K. Merz, N. Caesar and S. P. Verevkin, *ChemPhysChem*, 2015, **16**, 2890–2898.
14 R. L. Marchese Robinson, D. Geatches, C. Morris, R. Mackenzie, A. G. P. Maloney, K. J. Roberts, A. Moldovan, E. Chow, K. Pencheva and D. R. M. Vatvani, *J. Chem. Inf. Model.*, 2019, **59**, 4778–4792.
15 H. K. Buchholz and M. Stein, *J. Comput. Chem.*, 2018, **39**, 1335–1343.
16 S. L. Childs, G. P. Stahly and A. Park, *Mol. Pharmaceutics*, 2007, **4**, 323–338.
17 D. Braga, F. Grepioni, L. Maini, S. Prosperi, R. Gobetto and M. R. Chierotti, *Chem. Commun.*, 2010, **46**, 7715–7717.
18 D. Braga, F. Grepioni and O. Shemchuk, *CrystEngComm*, 2018, **20**, 2212–2220.
19 S. P. Kelley, A. Narita, J. D. Holbrey, K. D. Green, W. M. Reichert and R. D. Rogers, *Cryst. Growth Des.*, 2013, **13**, 965–975.
20 D. Yang, H. Wang, Q. Liu, P. Yuan, T. Chen, L. Zhang, S. Yang, Z. Zhou, Y. Lu and G. Du, *Chin. Chem. Lett.*, 2021, **33**, 3207–3211.
21 T. Alkhidir, Z. M. Saeed, A. F. Shunnar, E. Abujami, R. M. Nyadzayo, B. Dhokale and S. Mohamed, *Cryst. Growth Des.*, 2022, **22**, 485–496.
22 M. Gryl, M. Kozieł and K. M. Stadnicka, *Acta Crystallogr., Sect. B: Struct. Sci., Cryst. Eng. Mater.*, 2019, **75**, 53–58.

23 N. K. Duggirala, M. L. Perry, Ö. Almarsson and M. J. Zaworotko, *Chem. Commun.*, 2016, **52**, 640–655.
24 S. Aitipamula, R. Banerjee, A. K. Bansal, K. Biradha, M. L. Cheney, A. R. Choudhury, G. R. Desiraju, A. G. Dikundwar, R. Dubey, N. Duggirala, P. P. Ghogale, S. Ghosh, P. K. Goswami, N. R. Goud, R. R. K. R. Jetti, P. Karpinski, P. Kaushik, D. Kumar, V. Kumar, B. Moulton, A. Mukherjee, G. Mukherjee, A. Myerson, V. Puri, A. Ramanan, T. Rajamannar, C. M. Reddy, N. Rodriguez-Hornedo, R. D. Rogers, T. N. G. Row, P. Sanphui, N. Shan, G. Shete, A. Singh, C. C. Sun, J. A. Swift, R. Thaimattam, T. S. Thakur, R. K. Thaper, S. Thomas, S. Tothadi, V. R. Vangala, N. Variankaval, P. Vishweshwar, D. R. Weyna and M. J. Zaworotko, *Cryst. Growth Des.*, 2012, **12**, 2147–2152.
25 D. J. Berry and J. W. Steed, *Adv. Drug Delivery Rev.*, 2017, **117**, 3–24.
26 E. Grothe, H. Meekes, E. Vlieg, J. H. ter Horst and R. de Gelder, *Cryst. Growth Des.*, 2016, **16**, 3237–3243.
27 S. Guerin, S. Khorasani, M. Gleeson, J. O'Donnell, R. Sanii, R. Zwane, A. M. Reilly, C. Silien, S. A. M. Tofail, N. Liu, M. Zaworotko and D. Thompson, *Cryst. Growth Des.*, 2021, **21**, 5818–5827.
28 J. Nath and J. B. Baruah, *Cryst. Growth Des.*, 2021, **21**, 5325–5341.
29 W. Gong, P. K. Mondal, S. Ahmadi, Y. Wu and S. Rohani, *Int. J. Pharm.*, 2021, **608**, 121063.
30 T. A. Hegde, A. Dutta, T. C. Sabari Girisun and G. Vinitha, *Chem. Phys. Lett.*, 2021, **781**, 138971.
31 A. Kiguchiya, R. Teraoka, T. Sakane and E. Yonemochi, *Chem. Pharm. Bull.*, 2019, **67**, 945–952.
32 L. Zhao, M. P. Hanrahan, P. Chakravarty, A. G. DiPasquale, L. E. Sirois, K. Nagapudi, J. W. Lubach and A. J. Rossini, *Cryst. Growth Des.*, 2018, **18**, 2588–2601.
33 W. Ji, B. Xue, S. Bera, S. Guerin, L. J. Shimon, Q. Ma, S. A. Tofail, D. Thompson, Y. Cao, W. Wang and E. Gazit, *Mater. Today*, 2021, **42**, 29–40.
34 P. Vaňkátová, A. Kubíčková and K. Kalíková, *J. Chromatogr. A*, 2022, **1673**, 463074.
35 C. C. Da Silva and F. T. Martins, *RSC Adv.*, 2015, **5**, 20486–20490.
36 P. Rajasekar, C. Jose, M. Sarkar and R. Boomishankar, *Angew. Chem., Int. Ed.*, 2021, **60**, 4023–4027.
37 L. Zeng, Q. Yi, Q. Liu, K. Tang and B. van der Bruggen, *Sep. Purif. Technol.*, 2021, **257**, 117884.
38 V. Gore, D. Datta, M. Gadakar, K. Pokharkar, V. Mankar and S. Wavhal, *WO Pat.*, WO2009122215, 2009.
39 V. Gore, D. Datta, M. Gadakar, K. Pokharkar, V. Mankar and S. Wavhal, *US Pat.*, US20110124909, 2011.
40 B. S. Pradhan, *IN Pat.*, IN2010CH01584, 2010.
41 A. Khaja, V. S. R. Potla, S. Govind, B. R. Konudula, Y. K. Chauhan and D. Datta, *WO Pat.*, WO2009125427, 2009.
42 K. B. Mafatlal, K. N. Kagathara, K. Sivaprasad, P. C. Rajendra, V. P. Bhikhalal, B. U. Rajaram and M. I. Ambalal, *IN Pat.*, IN2009MU01587, 2009.
43 S. R. D. Reddy, S. R. Velivela and R. R. V. Reddy, *IN Pat.*, IN2010CH00299, 2010.
44 R. K. Thaper, M. D. Prabhavat, S. K. Arora, Y. D. Pawar, D. K. P. Varma, V. S. Kamble and V. S. Shinde, *IN Pat.*, IN2008KO00929, 2008.
45 D. K. Baidya, A. Agarwal, P. Khanna and M. K. Arora, *J. Anaesthesiol., Clin. Pharmacol.*, 2011, **27**, 307–314.
46 M. J. Brodie, *Epilepsia*, 2004, **45**(Suppl 6), 19.
47 C. A. Federico, J. S. Mogil, T. Ramsay, D. A. Fergusson and J. Kimmelman, *Pain*, 2020, **161**, 684–693.
48 N. M. Gajraj, *Anesth. Analg.*, 2007, **105**, 1805–1815.
49 D. R. Guay, *Am. J. Geriatr. Pharmacother.*, 2005, **3**, 274–287.
50 R. Kavoussi, *Eur. Neuropsychopharmacol.*, 2006, **16**(Suppl 2), S128–S133.
51 N. Kumar, A. Laferriere, J. S. C. Yu, A. Leavitt and T. J. Coderre, *J. Neurochem.*, 2010, **113**, 552–561.
52 B. A. Lauria-Horner and R. B. Pohl, *Expert Opin. Invest. Drugs*, 2003, **12**, 663–672.
53 R. A. Moore, S. Straube, P. J. Wiffen, S. Derry and H. J. McQuay, *Cochrane Database Syst. Rev.*, 2009, **3**, CD007076.
54 P. Ryvlin, E. Perucca and S. Rheims, *Neuropsychiatr. Dis. Treat.*, 2008, **4**, 1211–1224.
55 L. Zvejniece, E. Vavers, B. Svalbe, G. Veinberg, K. Rizhanova, V. Liepins, I. Kalvinsh and M. Dambrova, *Pharmacol., Biochem. Behav.*, 2015, **137**, 23–29.
56 I. Lapin, *CNS Drug Rev.*, 2001, **7**, 471–481.
57 M. Dambrova, L. Zvejniece, E. Liepinsh, H. Cirule, O. Zharkova, G. Veinberg and I. Kalvinsh, *Eur. J. Pharmacol.*, 2008, **583**, 128–134.
58 M. A. Downes, I. L. Berling, A. Mostafa, J. Grice, M. S. Roberts and G. K. Isbister, *Clin. Toxicol.*, 2015, **53**, 636–638.
59 Y. B. Joshi, S. F. Friend, B. Jimenez and L. R. Steiger, *J. Clin. Psychopharmacol.*, 2017, **37**, 478–480.
60 W. Li and B. Madhira, *Am. J. Ther.*, 2017, **24**, e639–e640.
61 D. J. McCabe, S. A. Bangh, A. M. Arens and J. B. Cole, *Am. J. Emerg. Med.*, 2019, **37**, 2066–2071.
62 D. R. Owen, D. M. Wood, J. R. H. Archer and P. I. Dargan, *Drug Alcohol Rev.*, 2016, **35**, 591–596.
63 B. Samas, W. Wang and D. B. Godrej, *Acta Crystallogr., Sect. E: Struct. Rep. Online*, 2007, **63**, o3938–o3938.
64 *CrysAlisPRO*, Oxford Diffraction/Agilent Technologies UK Ltd, Yarnton, England.
65 G. M. Sheldrick, *Acta Crystallogr., Sect. A: Found. Crystallogr.*, 2008, **64**, 112–122.
66 G. M. Sheldrick, *Acta Crystallogr., Sect. C: Struct. Chem.*, 2015, **71**, 3–8.
67 O. V. Dolomanov, L. J. Bourhis, R. J. Gildea, J. A. K. Howard and H. Puschmann, *J. Appl. Crystallogr.*, 2009, **42**, 339–341.
68 C. F. Macrae, I. Sovago, S. J. Cottrell, P. T. A. Galek, P. McCabe, E. Pidcock, M. Platings, G. P. Shields, J. S. Stevens, M. Towler and P. A. Wood, *J. Appl. Crystallogr.*, 2020, **53**, 226–235.
69 P. Giannozzi, O. Baseggio, P. Bonfà, D. Brunato, R. Car, I. Carnimeo, C. Cavazzoni, S. de Gironcoli, P. Delugas, F. Ferrari Ruffino, A. Ferretti, N. Marzari, I. Timrov, A. Urru and S. Baroni, *Chem. Phys.*, 2020, **152**, 154105.
70 *Physicians' desk reference 2007*, ed. Thomson P. D. R., Thomson PDR, Mondvale, NJ, 2007.

71 G. Kortüm, W. Vogel and K. Andrussow, *Pure Appl. Chem.*, 1960, **1**, 187–536.
72 D. Mootz and M. Schilling, *J. Am. Chem. Soc.*, 1992, **114**, 7435–7439.
73 R. M. Zelle, E. de Hulster, W. A. van Winden, P. de Waard, C. Dijkema, A. A. Winkler, J.-M. A. Geertman, J. P. van Dijken, J. T. Pronk and A. J. A. van Maris, *Appl. Environ. Microbiol.*, 2008, **74**, 2766–2777.
74 Chemicalize was used for prediction of pKa properties, 09/2022, https://chemicalize.com/ developed by ChemAxon (**http://www.chemaxon.com**).
75 T. Steiner, *Angew. Chem., Int. Ed.*, 2002, **41**, 48–76.
76 E. Batisai, A. Ayamine, O. E. Y. Kilinkissa and N. B. Báthori, *CrystEngComm*, 2014, **16**, 9992–9998.
77 K. A. Chu and S. H. Yalkowsky, *Int. J. Pharm.*, 2009, **373**, 24–40.
78 G. L. Perlovich, *Cryst. Growth Des.*, 2021, **21**, 5058–5071.
79 M. Banik, S. P. Gopi, S. Ganguly and G. R. Desiraju, *Cryst. Growth Des.*, 2016, **16**, 5418–5428.
80 S. J. Bethune, N. Huang, A. Jayasankar and N. Rodríguez-Hornedo, *Cryst. Growth Des.*, 2009, **9**, 3976–3988.
81 D. J. Good and N. Rodríguez-Hornedo, *Cryst. Growth Des.*, 2009, **9**, 2252–2264.
82 D. J. Good and N. Rodríguez-Hornedo, *Cryst. Growth Des.*, 2010, **10**, 1028–1032.
83 S. Kaya and C. Kaya, *Inorg. Chem.*, 2015, **54**, 8207–8213.
84 S. Kaya, A. Robles-Navarro, E. Mejía, T. Gómez and C. Cardenas, *J. Phys. Chem. A*, 2022, **126**, 4507–4516.
85 D. Komisarek, M. Pallaske and V. Vasylyeva, *Z. Anorg. Allg. Chem.*, 2021, **647**, 984–991.
86 M. Herbst, D. Komisarek, T. Strothmann and V. Vasylyeva, *Crystals*, 2022, **12**, 1393.